Conductivity Noise in Transmembrane Ion Channels Due to Ion Concentration Fluctuations via Diffusion

Don-On Daniel Mak* and Watt W. Webb#
*Physics Department, #School of Applied and Engineering Physics, Cornell University, Ithaca, New York 14853 USA

ABSTRACT A Green's function approach is developed from first principles to evaluate the power spectral density of conductance fluctuations caused by ion concentration fluctuations via diffusion in an electrolyte system. This is applied to simple geometric models of transmembrane ion channels to obtain an estimate of the magnitude of ion concentration fluctuation noise in the channel current. Pure polypeptide alamethicin forms stable ion channels with multiple conductance states in artificial phospholipid bilayers isolated onto tips of micropipettes with gigaohm seals. In the single-channel current recorded by voltage-clamp techniques, excess noise was found after the background instrumental noise and the intrinsic Johnson and shot noises were removed. The noise due to ion concentration fluctuations via diffusion was isolated by the dependence of the excess current noise on buffer ion concentration. The magnitude of the concentration fluctuation noise derived from experimental data lies within limits estimated using our simple geometric channel models. Variation of the noise magnitude for alamethicin channels in various conductance states agrees with theoretical prediction.

INTRODUCTION

Concentration fluctuations via random diffusion are found in any system in which diffusion is present. Such concentration fluctuations have been used in various kinds of fluctuation or concentration correlation spectroscopy (Madge et al., 1972; Feher and Weissman, 1973; Elson and Madge, 1974; Weissman, 1981), including fluorescence correlation spectroscopy (Madge et al., 1972), to study the mobility of particles (Elson and Webb, 1975; Weissman et al., 1976). In a conducting system, fluctuations in the local concentration of charge carriers via diffusion result in fluctuations in the local conductivity of the medium (Richardson, 1950; van Vliet and Fassett, 1965). These conductivity fluctuations give rise to fluctuations in the conductance of the conducting system that is detectable as current noise when a current is driven through the conducting system. The effect of such fluctuations is most conspicuous when the charge carrier concentration in the system is low, as in semiconductors; or when the conductance of the system is controlled by carrier concentration in a small region (Lax and Mengert, 1960), like contact regions between two conductors that are otherwise separated by an insulating layer, where the current flux is high, so that local conductivity fluctuations are effectively amplified. This contact noise has been investigated extensively over a long time (Richardson, 1950; Weissman, 1975; Vandamme, 1976) as a possible cause of the ubiquitous $1/f$ noise found in a wide range of conducting systems (Hooge, 1976; Weissman, 1988).

In our study of the noise in the current passing under constant applied potential through individual channels formed by the polypeptide alamethicin (Mak and Webb, 1995a,b) in artificial lipid bilayers using "patch-clamp" techniques (Hamill et al., 1981), we found excess current noise above the theoretical Johnson (Nyquist, 1928) and shot noise level (DeFelice, 1981; Laüger, 1975). It has been suggested that part of the excess noise is due to fluctuations in the channel conductance caused by ion concentration fluctuations via diffusion in and around the channel (Bezrukov et al., 1989; Bezrukov and Vodyanoy, 1991, 1994).

Although conductivity fluctuation is a fundamental process present in all conducting systems, previous investigations of this process (Hooge, 1969, 1972; Hooge and Hoppenbrouwers, 1969; Hoppenbrouwers and Hooge, 1970; Hooge and Gaal, 1971; Honig 1974; Weissman, 1975; Vandamme, 1976) did not develop an evaluation of the magnitude of this noise from first principles that is appropriate for the mesoscopic conducting system of a protein channel in a lipid bilayer. Therefore, in the first part of this paper, based on previous studies of carrier concentration fluctuations (Richardson, 1950; van Vliet and Fassett, 1965; Weissman, 1975), we develop a Green's function approach to deriving from first principles the power spectral density (PSD) of the fluctuations in the resistance of an electrolyte system caused by ion concentration fluctuations via random diffusion (Basic Theory). This approach is applied to geometric models of a transmembrane ion channel to obtain theoretical estimates of the channel current noise caused by ion concentration fluctuations (Theoretical Ion Concentration Fluctuations in Channels). These theoretical estimates are compared to the magnitude of the current noise in alamethicin channels that is attributed to ion concentration fluctuations (Ion Concentration Fluctuations in Alamethicin Channels).

Received for publication 10 April 1996 and in final form 20 December 1996.

Address reprint requests to Dr. Don-On Daniel Mak, Physiology Department, University of Pennsylvania, Room 314, Stellar-Chance Labs, 422 Curie Blvd., Philadelphia, PA 19104. Tel.: 215-898-0468; Fax: 215-573-8590; E-mail: dmak@mail.med.upenn.edu.

0006-3495/97/03/1153/12 $2.00

BASIC THEORY

In this section we will derive the PSD of the resistance fluctuations caused by electrolyte concentration fluctuations due to ion diffusion in terms of Green's functions in an approach similar to that used by van Vliet and Fassett (1965). We use the following notations. For a quantity $A(t)$ with time dependence, $\langle A\rangle$ is $A(t)$ averaged over time and the fluctuation $\Delta A(t) = A(t) - \langle A\rangle$. For a quantity $x(\vec{\mathbf{r}}, t)$ with spatial and time dependence, $\bar{x}$ is $x(\vec{\mathbf{r}}, t)$ averaged over both $\vec{\mathbf{r}}$ and t, $\Delta x(\vec{\mathbf{r}}, t) = x(\vec{\mathbf{r}}, t) - \bar{x}$. $\langle \Delta A(t)\Delta A(0)\rangle$ is the correlation function of $\Delta A(t + \tau)\Delta A(\tau)$ averaged over all values of τ. The PSD $S_A(\omega)$ is the one-sided spectral density (Press et al., 1987a) of $\Delta A(t)$.

For simplicity, we consider the case of current passing through a continuous electrolyte with a uniform mean conductivity $\bar{\sigma}$. The field intensity $\vec{\mathbf{E}}(\vec{\mathbf{r}})$ in the medium is low enough at any point in the medium that Ohm's law, $\vec{\mathbf{E}}(\vec{\mathbf{r}})\ \sigma(\vec{\mathbf{r}}, t) = \vec{\mathbf{J}}(\vec{\mathbf{r}}, t)$, is valid. The electric field is time-invariant. The electrolyte contains one kind of salt with monovalent ions only (like NaCl). Ion concentration in the medium is low enough that the electrolyte is completely ionized and Kohlrausch's law of independent migration of ions applies (Creighton, 1944):

$$\sigma(\vec{\mathbf{r}}, t) = F(u_- + u_+)\ \rho(\vec{\mathbf{r}}, t), \tag{1}$$

where u_+ and u_- are the mobilities of the cation and anion species in the electrolyte, F is Faraday's number, and $\rho(\vec{\mathbf{r}}, t)$ is the local electrolyte concentration.

Spontaneous ion concentration fluctuations via random thermal diffusion of ions inside the medium cause fluctuations in the local conductivity in the medium, which in turn cause fluctuations in the resistance of the whole electrolyte system. If a constant applied potential V is maintained across the system, the conductivity fluctuations in the medium will cause fluctuations in the current passing through the system. Considering the power dissipation in the electrolyte (Richardson, 1950; Weissman, 1975), and ignoring higher-order terms,

$$\Delta R(t) = \frac{-\langle R\rangle^2}{V^2}\int \Delta\sigma(\vec{\mathbf{r}}, t)\mathbf{E}^2(\vec{\mathbf{r}})\ \mathrm{d}^3\vec{\mathbf{r}}. \tag{2}$$

The resistance autocorrelation function is

$$\langle \Delta R(t)\Delta R(0)\rangle = \frac{1}{\langle I\rangle^4}\iint \mathbf{E}^2(\vec{\mathbf{r}})\mathbf{E}^2(\vec{\mathbf{r}}') \cdot \langle \Delta\sigma(\vec{\mathbf{r}}, t)\Delta\sigma(\vec{\mathbf{r}}', 0)\rangle\ \mathrm{d}^3\vec{\mathbf{r}}\ \mathrm{d}^3\vec{\mathbf{r}}', \tag{3}$$

where $\langle I\rangle = V/\langle R\rangle$. The volume integral in Eq. 3 is very similar to the one used in fluorescence correlation spectroscopy (Madge et al., 1972; Elson and Webb, 1975), in which the intensity of the incident laser light replaces the local electric field intensity and the correlation of the fluctuations in fluorescent dye concentration replaces the correlation of the conductivity fluctuations.

The Green's function $g(\vec{\mathbf{r}}, t; \vec{\mathbf{r}}')$ of the transport differential operator of the system under consideration is defined as in van Vliet and Fassett (1965), so that

$$\langle \Delta\rho(\vec{\mathbf{r}}, t)\Delta\rho(\vec{\mathbf{r}}', 0)\rangle = \int \mathrm{d}^3\vec{\mathbf{r}}''g(\vec{\mathbf{r}}, t; \vec{\mathbf{r}}'')\langle \Delta\rho(\vec{\mathbf{r}}'', 0)\Delta\rho(\vec{\mathbf{r}}', 0)\rangle. \tag{4}$$

For our experimental buffers (0.33–2 M NaCl), the Debye screening length $\kappa \approx 2.1$–5.0 Å (Bezrukov et al., 1989). For ion transport processes around a transmembrane ion channel with a length of ~40 Å under such ionic concentrations, it is appropriate to use the approximation (Lax and Mengert, 1960; van Vliet and Fassett, 1965)

$$\langle \Delta\rho(\vec{\mathbf{r}}', 0)\Delta\rho(\vec{\mathbf{r}}'', 0)\rangle = \bar{\rho}\delta(\vec{\mathbf{r}}' - \vec{\mathbf{r}}''), \tag{5}$$

where $\delta(\vec{\mathbf{r}}' - \vec{\mathbf{r}}'')$ is the standard delta function.

Using the Wiener-Khintchine theorem, the PSD $S_R(\omega)$ of the resistance fluctuation is defined in terms of the autocorrelation function:

$$S_R(\omega) = 2\int_{-\infty}^{\infty} e^{i\omega t}\langle \Delta R(t)\Delta R(0)\rangle \mathrm{d}t. \tag{6}$$

Putting Eqs. 1, 3, 4 and 5 into Eq. 6,

$$S_R(\omega) = \frac{2\bar{\sigma}^2}{\bar{\rho}\langle I\rangle^4}\iint \mathrm{d}^3\vec{\mathbf{r}}\ \mathrm{d}^3\vec{\mathbf{r}}'\mathbf{E}^2(\vec{\mathbf{r}})\mathbf{E}^2(\vec{\mathbf{r}}')\int_{-\infty}^{\infty} e^{i\omega t}g(\vec{\mathbf{r}}, t; \vec{\mathbf{r}}')\mathrm{d}t. \tag{7}$$

The Laplace transform $G(\vec{\mathbf{r}}, -i\omega; \vec{\mathbf{r}}')$ of $g(\vec{\mathbf{r}}, t; \vec{\mathbf{r}}')$ is defined as (van Vliet and Fassett, 1965)

$$G(\vec{\mathbf{r}}, -i\omega; \vec{\mathbf{r}}') = \int_0^{\infty} e^{i\omega t}g(\vec{\mathbf{r}}, t; \vec{\mathbf{r}}')\mathrm{d}t. \tag{8}$$

Because $g(\vec{\mathbf{r}}, -t; \vec{\mathbf{r}}') = g(\vec{\mathbf{r}}', t; \vec{\mathbf{r}})$ for a stationary system and Eq. 7 is symmetrical for $\vec{\mathbf{r}}$ and $\vec{\mathbf{r}}'$, $S_R(\omega)$ can be expressed in terms of $G(\vec{\mathbf{r}}, i\omega; \vec{\mathbf{r}}')$,

$$S_R(\omega) = \frac{4\bar{\sigma}^2}{\langle I\rangle^4\bar{\rho}}\Re\left[\iint \mathrm{d}^3\vec{\mathbf{r}}\ \mathrm{d}^3\vec{\mathbf{r}}'\mathbf{E}^2(\vec{\mathbf{r}})\mathbf{E}^2(\vec{\mathbf{r}}')G(\vec{\mathbf{r}}, i\omega; \vec{\mathbf{r}}')\right], \tag{9}$$

where $\Re[z]$ represents the real part of z.

For low-frequency concentration fluctuations, charge neutrality is maintained with essentially complete correlation between the cation and anion concentration fluctuations. Effects of separation of charges only become significant for those fluctuations with frequencies $\omega > D\kappa^{-2}$, where D is the diffusion coefficient of the ions and κ is the Debye screening length (same as $1/\lambda$ in Lax and Mengert, 1960). For our aqueous buffer, $D \approx 2 \times 10^{-9}\ \mathrm{m^2 s^{-1}}$, $\kappa \approx 3 \times 10^{-10}$ m, so $D\kappa^{-2} \approx 2 \times 10^{10}\ \mathrm{s^{-1}}$, much higher than our experimental frequency range (≤20 kHz). The concentration fluctuations studied in our experiments are effec-

tively electrically neutral and are not detectably affected by the potential applied across the ion channel under our experimental conditions. The Na^+ ions in our two-ion experimental buffer always flow in an opposite direction from the Cl^- ions. Therefore, the ion flow cannot significantly transport the concentration fluctuations, which must obey charge neutrality. Thus the propagation of these concentration fluctuations detected by our experiment is mainly by diffusion. The appropriate Green's function $g(\vec{\mathbf{r}}, t; \vec{\mathbf{r}}')$ is the one that satisfies the diffusion transport equation, so $G(\vec{\mathbf{r}}, i\omega; \vec{\mathbf{r}}')$ is given by

$$\nabla^2_{\vec{\mathbf{r}}} G(\vec{\mathbf{r}}, i\omega; \vec{\mathbf{r}}') + \left(\frac{-i\omega}{D}\right) G(\vec{\mathbf{r}}, i\omega; \vec{\mathbf{r}}') = \frac{-1}{D}\,\delta(\vec{\mathbf{r}} - \vec{\mathbf{r}}'). \tag{10}$$

By definition, $G(\vec{\mathbf{r}}, i\omega; \vec{\mathbf{r}}')$ must satisfy the same spatial boundary conditions as $g(\vec{\mathbf{r}}, t; \vec{\mathbf{r}}')$.

Equation 10 is similar to the equation satisfied by the Green's function $G_k(\vec{\mathbf{r}}|\vec{\mathbf{r}}')$ of the inhomogeneous Helmholtz equation (Morse and Feshbach, 1953),

$$\nabla^2 G_k(\vec{\mathbf{r}}|\vec{\mathbf{r}}') + k^2 G_k(\vec{\mathbf{r}}|\vec{\mathbf{r}}') = -4\pi\delta(\vec{\mathbf{r}} - \vec{\mathbf{r}}'). \tag{11}$$

$G(\vec{\mathbf{r}}, i\omega; \vec{\mathbf{r}}')$ is a Green's function of the Helmholtz equation if

$$k^2 = -i\omega/D. \tag{12}$$

THEORETICAL ION CONCENTRATION FLUCTUATIONS IN CHANNELS

To apply the Green's function approach to obtain a resistance fluctuation PSD in a protein ion channel system, we must first find the electric field $\vec{\mathbf{E}}(\vec{\mathbf{r}})$ in the system. Then we have to find the Green's function $G(\vec{\mathbf{r}}, i\omega; \vec{\mathbf{r}}')$ that satisfies the boundary conditions for diffusion around the channel. Finally, the integration in Eq. 9 has to be performed. In the complex environment of a protein ion channel, each of these tasks is nontrivial and requires various simplifications to be assumed to keep the problem manageable.

In a protein ion channel, the channel pore has a complicated shape, determined by the conformation of the channel protein. So $\vec{\mathbf{E}}(\vec{\mathbf{r}})$ due to the external applied potential and the ion diffusion conditions are complicated. The charge distribution in the protein and the polar headgroups of the lipid bilayer (Latorre et al., 1992) in which the protein channel is located contributes to the local electric field (Jordan, 1986). In our approximation, the effect of these intrinsic electric fields and the interaction between the ions and the channel are expressed as energy barriers in the channel pore experienced by ions moving across the channel. Thus the volume of electrolyte in and around the channel can be divided into two kinds of regions:

1) In the region we will refer to as the "channel constriction" (Mak and Webb, 1995a) in the middle of the channel pore, the energy barriers allow only discrete movements of individual ions. Such discrete movement of ions over the barriers can give rise to a nonohmic relation between channel current and applied potential according to a model proposed by Laüger (1975). Because the continuous medium assumption for the electrolyte concentration fluctuations cannot be applied in this region, it is excluded from our evaluation of concentration fluctuation noise. Current noise arising from discrete ion movements in this region is evaluated separately in our consideration of channel shot noise (Mak and Webb, 1995b).

2) Outside the channel and in the regions on either side of the channel constriction that we will refer to as the "channel vestibules," there is little ion-channel interaction. In these regions, the continuous-medium assumption is applicable. These regions together contribute the ohmic spreading resistance to the total channel resistance (Mak and Webb, 1995a) and give rise to the Johnson noise in the channel current. These are also the regions in which thermal diffusion of ions generates ion concentration fluctuations.

Fluctuations in the spreading resistance: contact disc model

We use the contact disc model to estimate the concentration fluctuation noise for large-diameter channels. We assume that the channel pore is circular and the length of the channel is small compared with the size of the pore. Then we can represent the regions around the channel where ions move continuously (outside the channel and in the channel vestibules) by the simple and well-studied model of the pore as a contact disc connecting two semi-infinite bodies of electrolyte. Because of the vast simplifications used in our models, we expect to obtain just an order-of-magnitude estimate of the channel current noise caused by ion concentration fluctuations with our numerical evaluation.

The electric field and current distribution around a contact disc have been described in detail (Holm, 1967). Electrical noise in the spreading resistance around a contact disc with geometry similar to that of our model channel has been investigated before (Hooge and Gaal, 1971; Honig, 1974; Weissman, 1975; Vandamme, 1976). However, those studies were mainly concerned with $1/f$ noise. In some of them (Hooge and Gaal, 1971; Honig, 1974; Vandamme, 1976), an empirical $1/f$ spectrum (Hooge, 1969; Hooge and Hoppenbrouwers, 1969; Hoppenbrouwers and Hooge, 1970; Hooge, 1972) of unspecified origin was used as the PSD for the local conductivity fluctuations, whereas in others (Weissman, 1975), generation of $1/f$ noise from local conductivity fluctuations in the vicinity of the contact disc was considered. Because the current fluctuation PSDs observed in polypeptide ion channels are nearly white with little frequency dependence (Bezrukov et al., 1987; Mak and Webb, 1995b), we evaluate the resistance fluctuation PSD from first principles, assuming that it is caused by local ion concentration fluctuations in the electrolyte via random ion diffusion, following the Green's function approach outlined in the previous section.

The oblate spheroidal coordinate system (μ, θ, ϕ) (Morse and Feshbach, 1953) is appropriate for the contact disc model. The membrane is in the x–y plane, where the azimuthal angle $\theta = \pi/2$ and the channel is the contact disc of radius ε where $\mu = 0$. With the electrical potential given in (Holm, 1967),

$$\mathbf{E}^2(\vec{\mathbf{r}})\, \mathrm{d}^3\vec{\mathbf{r}} = \frac{\langle I\rangle^2}{(2\pi\bar{\sigma})^2\varepsilon}\frac{\sin\theta}{\cosh\mu}\,\mathrm{d}\mu\,\mathrm{d}\theta\,\mathrm{d}\phi. \tag{13}$$

Substituting Eq. 13 into Eq. 9,

$$S_{\mathrm{R}}(\omega) = \frac{1}{4\bar{\sigma}^2\bar{\rho}\pi^4\varepsilon^2}\,\Re\left[\int_6 \frac{\sin\theta\sin\theta'}{\cosh\mu\cosh\mu'}\,G(\vec{\mathbf{r}}, i\omega; \vec{\mathbf{r}}')\,\mathrm{d}V_6\right], \tag{14}$$

where $\int_6 \mathrm{d}V_6$ denotes integration over the six dimensions of μ, μ', θ, θ', ϕ, ϕ' and the limits of the integral are the boundary of the electrolyte system.

In this simplified model of the ion channel as a contact disc, the membrane at $\theta = \pi/2$ is assumed to be totally impermeable to ions, whereas the contact disc at $\mu = 0$ allows free passage of ions. The Green's function satisfying this diffusion condition is complicated, as the permeability for ions across the x–y plane changes abruptly at the edge of the contact disc.

For a simple approximation of the Green's function, the electrolyte is divided into three regions: I, II, and III (Fig. 1). I is $(0 \le \mu < 1)$; II is $[(1 \le \mu < \infty) \wedge (0 \le \theta < \pi/2)]$; and III is $[(1 \le \mu < \infty) \wedge (\pi/2 < \theta \le \pi)]$. When $\vec{\mathbf{r}}$ and $\vec{\mathbf{r}}'$ are both far from the contact disc and on the same side of the membrane (i.e., both $\vec{\mathbf{r}}$ and $\vec{\mathbf{r}}' \in$ II or III), the impermeable membrane dominates. When $\vec{\mathbf{r}}$ and $\vec{\mathbf{r}}'$ are far from the contact disc but on opposite sides of the membrane (i.e., $\vec{\mathbf{r}} \in$ II and $\vec{\mathbf{r}}' \in$ III or vice versa), the two points are effectively isolated by the membrane, so that $\langle \Delta\sigma(\vec{\mathbf{r}}, t)\Delta\sigma(\vec{\mathbf{r}}', t)\rangle = 0$. When either $\vec{\mathbf{r}}$ or $\vec{\mathbf{r}}' \in$ I (i.e., near the contact disc), the disc permits free movement of ions across the x–y plane.

The Green's function of the inhomogeneous Helmholtz equation in an infinite, three-dimensional medium with unrestricted ion diffusion is (Morse and Feshbach, 1953)

$$G(\vec{\mathbf{r}}, i\omega; \vec{\mathbf{r}}') = \frac{1}{4\pi D}\frac{\exp(ikQ\varepsilon)}{Q\varepsilon}, \tag{15}$$

where $Q = |\vec{\mathbf{r}} - \vec{\mathbf{r}}'|/\varepsilon$ is dimensionless and k is defined in Eq. 12. The constant term $(4\pi D)^{-1}$ is derived by comparing Eqs. 10 and 11.

For both $\vec{\mathbf{r}}$ and $\vec{\mathbf{r}}' \in$ I, substituting Eq. 15 into Eq. 14 gives

$$S_{\mathrm{R}}^{\mathrm{I}}(\omega) = \Xi\left[\int_0^1 \mathrm{d}\mu \int_0^1 \mathrm{d}\mu' \int_0^\pi \mathrm{d}\theta \int_0^\pi \mathrm{d}\theta' \int_0^{2\pi} \mathrm{d}\phi \int_0^{2\pi} \mathrm{d}\phi'\, \Upsilon(\vec{\mathbf{r}}, \vec{\mathbf{r}}')\right], \tag{16}$$

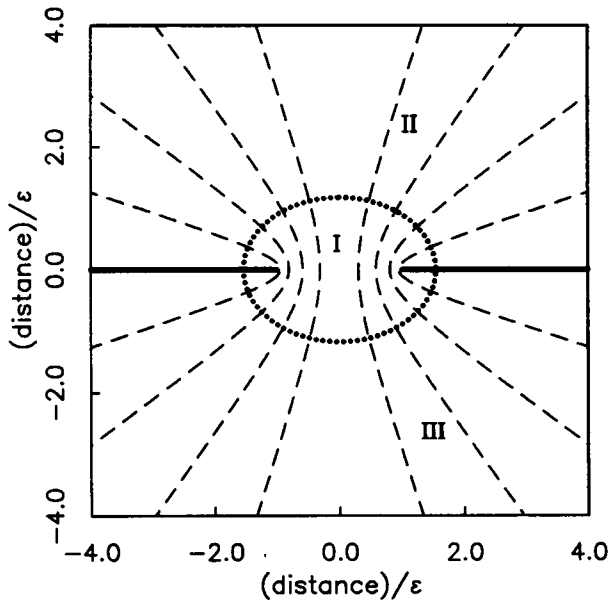

FIGURE 1 Schematic diagram of a model channel as a contact disc showing a cross section of the model channel in the x–z plane. The vertical axis is the z axis and the horizontal axis is the x axis. The solid lines are $\theta = \pi/2$ and $\mu > 0$, representing the impermeable membrane, where (μ, θ, ϕ) are the oblate spheroidal coordinates. The dotted line is $\mu = 1$, representing the boundary for region I. Region II has $1 \le \mu \wedge 0 \le \theta < \pi/2$. Region III has $1 \le \mu \wedge \pi/2 < \theta \le \pi$. The dashed lines are typical field lines in the electrolyte. The oblate spheroidal coordinates (μ, θ, ϕ) are related to the Cartesian coordinates (x, y, z) by $x = \varepsilon\cos\phi\sin\theta\cosh\mu$; $y = \varepsilon\sin\phi\sin\theta\cosh\mu$; $z = \varepsilon\cos\theta\sinh\mu$, where ε is a scale term.

where

$$\Xi = \left(\frac{1}{D\bar{\rho}}\right)\left(\frac{1}{16\pi^5\bar{\sigma}^2\varepsilon^3}\right), \tag{17}$$

$$\Upsilon(\vec{\mathbf{r}}, \vec{\mathbf{r}}') = \frac{\sin\theta\sin\theta'}{\cosh\mu\cosh\mu'}\,\frac{\cos(\hat{\omega}Q)}{Q\exp(\hat{\omega}Q)}, \tag{18}$$

$$\hat{\omega} = \sqrt{\omega\varepsilon^2/2D} = \sqrt{\omega/\omega_0}. \tag{19}$$

$\hat{\omega}$ is the dimensionless reduced frequency and ω_0 is the reference frequency determined by the channel radius ε.

Similarly, the resistance fluctuation spectrum $S_{\mathrm{R}}^{\times}(\omega)$ for $\vec{\mathbf{r}} \in$ I and $\vec{\mathbf{r}}' \notin$ I is

$$S_{\mathrm{R}}^{\times}(\omega) = \Xi\left[\int_0^1 \mathrm{d}\mu \int_1^\infty \mathrm{d}\mu' \int_0^\pi \mathrm{d}\theta \int_0^\pi \mathrm{d}\theta' \int_0^{2\pi} \mathrm{d}\phi \int_0^{2\pi} \mathrm{d}\phi'\, \Upsilon(\vec{\mathbf{r}}, \vec{\mathbf{r}}')\right]. \tag{20}$$

By symmetry, the case where $\vec{\mathbf{r}}' \in$ I and $\vec{\mathbf{r}} \notin$ I gives the same contribution to the resistance fluctuations.

For $\vec{\mathbf{r}}$ and $\vec{\mathbf{r}}' \in$ II, the x–y plane appears impermeable to the ions, so diffusion of ions is limited to θ and θ' between 0 and $\pi/2$. With this boundary condition, the method of images (Morse and Feshbach, 1953) is applicable. Using

symmetry of the Green's function w.r.t. the x–y plane,

$$S_R^{II}(\omega) = \frac{\Xi}{2}\left[\int_1^\infty d\mu \int_1^\infty d\mu' \int_0^\pi d\theta \int_0^\pi d\theta' \int_0^{2\pi} d\phi \int_0^{2\pi} d\phi' \, \Upsilon(\vec{r}, \vec{r}')\right]. \quad (21)$$

By symmetry, $S_R^{III}(\omega)$, when both $\vec{r}$ and $\vec{r}' \in$ III, must have the same magnitude.

Assuming that resistance fluctuations in various regions of the electrolyte are not correlated, the total resistance fluctuation spectrum is

$$S_R(\omega) \approx S_R^{I}(\omega) + 2S_R^{\times}(\omega) + 2S_R^{II}(\omega) \approx \Xi\left[\int_0^\infty d\mu \int_0^\infty d\mu' \int_0^\pi d\theta \int_0^\pi d\theta' \int_0^{2\pi} d\phi \int_0^{2\pi} d\phi' \, \Upsilon(\vec{r}, \vec{r}')\right]. \quad (22)$$

Using Ohm's law and the average resistance of a contact disc (Holm, 1967) and Eq. 17, we obtain the normalized fluctuation PSD due to ion concentration fluctuations:

$$S^{ion}(\omega) = \frac{S_R(\omega)}{\langle R\rangle^2} = \frac{S_I(\omega)}{\langle I\rangle^2} \approx \frac{1}{\bar{\rho}D}\frac{1}{4\pi^5\varepsilon} \cdot \left[\int_0^\infty d\mu \int_0^\infty d\mu' \int_0^\pi d\theta \int_0^\pi d\theta' \int_0^{2\pi} d\phi \int_0^{2\pi} d\phi' \, \Upsilon(\vec{r}, \vec{r}')\right]. \quad (23)$$

The factor $1/\bar{\rho}$ in $S^{ion}(\omega)$ comes from Eq. 9, and the factor $1/D$ comes from the form of Eq. 10. Both are independent of the form of the Green's function $G(\vec{r}, i\omega; \vec{r}')$, which is controlled by the channel geometry.

Because the integral in Eq. 23 has no analytical solution, its value was estimated using numerical methods. Rotational symmetry about the z axis reduces the integral to five dimensions (Carslaw and Jaeger, 1948). A simple computer algorithm applying the extended Simpson's rule (Press et al., 1987b) with 30–60 intervals in each dimension provides the necessary order-of-magnitude estimate. With 60 intervals, at the low-frequency limit ($\omega \ll \omega_0$), a 33% increase in interval number in each dimension causes <1% change in the value of the integral.

The form of the integrand $\Upsilon(\vec{r}, \vec{r}')$ in Eq. 18 suggests that there are unintegrable singularities at $\vec{r} \to \vec{r}'$ where $Q^{-1} \to \infty$. Such singularities are the property of the Green's function. The singularities do not occur in reality because the continuous medium approximation we assumed fails when the distance εQ is comparable to the diameter $2a$ of the ions (the value of the ionic radius a may not be well defined because of the hydration shells of ions and long-range ion-ion interactions). For $\varepsilon Q < 2a$, there is no correlation of electrolyte number density fluctuations at $\vec{r}$ and $\vec{r}'$ by the diffusion process. Q in the integral should be limited to $Q > 2a/\varepsilon$. In the case of a typical protein channel, $2a/\varepsilon \approx 0.1$–$1$. With this physical cut-off, $\Upsilon(\vec{r}, \vec{r}')$ in the integral does not generate any singularities.

In large channels with pore radii significantly larger than the physical size of the ions ($\varepsilon \gg 2a$), the physical cut-off no longer affects the value of the integral in Eq. 23 significantly as the channel increases in size. Then the value of the integral is effectively independent of channel size. From Eq. 23, the normalized fluctuation PSD of large channels scales according to the relation $S^{ion}(\omega) \propto \varepsilon^{-1}$.

Fluctuations in the channel pore resistance: tube model

As the channel radius decreases, the contact disc becomes a less appropriate model for the regions of electrolyte with continuous ion movement, especially as the resistance of the electrolyte inside the channel vestibules becomes the major contribution to $S_R(\omega)$. To estimate the magnitude of the fluctuations in the resistance from the channel vestibules, we use the "tube model." In this model we consider the extreme situation in which all of the ion concentration fluctuation noise arises from fluctuations in the resistance of the electrolyte inside the channel vestibules, and the spreading resistance of electrolyte outside the channel is ignored. The electrolyte inside the channel vestibule is represented by a tube in which the electric field is uniform and parallel to the axis of the tube. Transverse diffusion of ions along any equipotential surface will not affect the conductance of the tube. Only diffusion of ions along the channel axis is relevant to generation of current noise by ion concentration fluctuations. Therefore, the shape of the channel cross section does not affect the magnitude of current noise caused by ion concentration fluctuations, as long as the cross-sectional area of the channel accessible to the ions is the same. For simplicity, we consider a rectangular tube of electrolyte.

In the case of a rectangular tube, the Cartesian coordinate system is appropriate. The model channel is bound by the planes $x = \pm\varepsilon$ and $y = \pm\varepsilon$, which are totally impermeable to ion diffusion. Ions can diffuse freely in the z direction. The electric field is parallel to the z axis and constant in magnitude throughout the channel of length ℓ. We consider the fluctuations in the resistance of the electrolyte between $z = 0$ and $z = \ell$ due to ion concentration fluctuations inside this tube. From the geometry of the model,

$$\mathbf{E}^2(\vec{r})\, d^3\vec{r} = \langle I\rangle^2 dx\, dy\, dz/(16\bar{\sigma}^2\varepsilon^4). \quad (24)$$

Defining $(x, y, z) = \varepsilon(x_0, y_0, z_0)$ and substituting Eq. 24 into Eq. 9,

$$S_R(\omega) = \frac{1}{64\bar{\sigma}^2\bar{\rho}\varepsilon^2}\Re\left[\int_0^{\ell/\varepsilon} dz_0 \int_0^{\ell/\varepsilon} dz_0' \int_{-1}^{1} dx_0 \int_{-1}^{1} dx_0' \int_{-1}^{1} dy_0 \int_{-1}^{1} dy_0' G(\vec{r}, i\omega; \vec{r}')\right]. \quad (25)$$

The Green's function is found using the method of images (Morse and Feshbach, 1953), but with infinite images generated by reflections w.r.t. the impermeable planes $x = \pm\varepsilon$ and $y = \pm\varepsilon$. Putting the appropriate Green's function into Eq. 25,

$$S^{\text{ion}}(\omega) = \frac{1}{D\bar{\rho}}\frac{\varepsilon}{16\pi\ell^2}\int_0^{\ell/\varepsilon} dz_0 \int_0^{\ell/\varepsilon} dz_0' \int_{-1}^{1} dx_0 \int_{-1}^{1} dy_0 \int_{-\infty}^{\infty} dx_0' \int_{-\infty}^{\infty} dy_0' \frac{\cos(\hat{\omega}Q)}{Q\exp(\hat{\omega}Q)}. \quad (26)$$

The limits for x_0', y_0' are $\pm\infty$ because of the infinite reflections. The six-dimensional integration is estimated numerically in a way similar to that used for the contact disc model.

ION CONCENTRATION FLUCTUATIONS IN ALAMETHICIN CHANNELS

Alamethicin channel current noise

Alamethicin, a well-studied polypeptide with 20 amino acid residues, is capable of forming well-defined, voltage-dependent channels with characteristic multiple conductance states in a wide range of biological membranes and synthetic lipid bilayers (Latorre and Alvarez, 1981; Sansom, 1991; Woolley and Wallace, 1992; Mak and Webb, 1995a) (Fig. 2). Because the conductance values of various conductance states are not integral multiples of one another (Eisenberg et al., 1977), the conductance states are not caused by multiple channels present at the same time in the bilayer, but are due to a single channel with an aqueous, ion-conducting pore that can have several different sizes, each pore size corresponding to a different conductance state. Under an applied transmembrane potential of the correct polarity (Mueller and Rudin, 1968; Cherry et al., 1972), alamethicin forms stable channels that last for long periods of time (Boheim, 1974), especially in phospholipid bilayers under low temperature (Gordon and Haydon, 1976), making it an excellent subject for our study of open-channel current noise, because many samples of current noise power spectra can be easily obtained when the channel stays in the same conductance state. Patch-clamp techniques (Hamill et al., 1981; Calahan and Neher, 1992) allow records with low background noise (Sigworth, 1985) to be made of ion currents passing under constant applied voltage through individual alamethicin channels in artificial lipid bilayers isolated at the tips of micropipettes with stable, gigaohm seals for extensive periods of time (minutes, even hours).

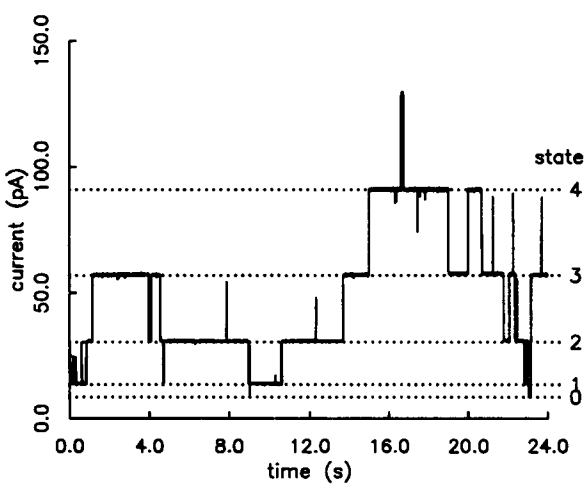

FIGURE 2 A typical current record of a typical channel (persistent) formed by purified alamethicin showing multiple conductance states (states 1–5). State 0 is the closed channel. The same experimental conditions as described by Mak and Webb (1995a) were used. The NaCl concentration in the buffer solution was 1.0 M. The temperature of the buffer solution was 7.0°C. Applied potential for this record was +44 mV. The record has been digitally filtered at 737.5 Hz for plotting purposes.

In our first paper describing our study of single-channel currents in alamethicin channels by patch-clamp techniques (Mak and Webb, 1995a), we reported that purified alamethicin can form two classes of channels: persistent channels that remain active for long periods (minutes to hours) and nonpersistent channels that stay active only briefly (less than a minute in most cases), each with a unique set of conductance states and different open-channel kinetic properties. To explain the nonohmic behavior of alamethicin channel currents under high applied potentials and the increase in channel current magnitude in higher conductance states, we proposed molecular models for the persistent and nonpersistent alamethicin channels based on the secondary structure of alamethicin determined by x-ray diffraction study (Fox and Richards, 1982). In our models, the ion-conducting channel pore has an hourglass shape with a narrow constriction about 3 Å in length formed by Gln side chains protruding into the channel pore from the alamethicin helices that form the wall of the channel pore. This constriction presents a single energy barrier over which ions move discretely, as described by Laüger (1975). Because the full length of the channel is ~35 Å (Schwarz and Savko, 1982), the channel constriction constitutes only a small portion of the total volume of the channel pore. On either side of this constriction, the electrolyte in the wider "vestibule" of the channel, together with the electrolyte outside the channel, generates an ohmic spreading resistance that is in series with the nonohmic resistance caused by the channel constriction.

In the second paper of this series (Mak and Webb, 1995b), we described the open-channel current noise of alamethicin channels. We demonstrated that between the observable frequency range of 100 Hz to 20 kHz, the channel current noise spectra for the various conductance states in both the persistent and nonpersistent channels are frequency independent within experimental error limits (Fig. 3). This indicates that the various sources contributing to the measured channel current noise do not have any significant frequency dependence within the experimental

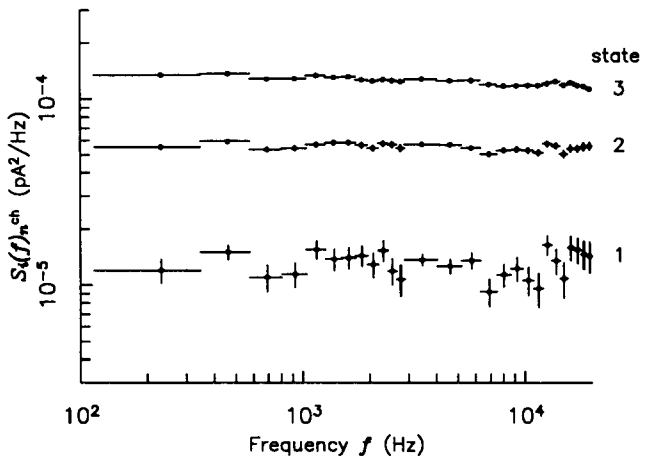

FIGURE 3 PSD $S_i(f)_n^{ch}$ of the fluctuation in current passing through a typical persistent alamethicin channel. The same experimental conditions were used in Fig. 2. The applied potential was +60 mV across the bilayer.

frequency range. Thus, a $1/f$ spectrum is not the appropriate form for local conductivity fluctuations around the channel. Because the channel current noise spectra are frequency independent, the magnitude of the channel current noise can be effectively represented by a characteristic PSD value obtained by averaging the channel current noise PSD over all frequencies between 100 Hz and 20 kHz.

Noise arising from short unresolved current pulses produced by the channel undergoing rapid transitions from conductance state n to state $(n \pm 1)$ and back to state n was estimated from dwell-time distribution histograms of the channel (Colquhoun and Sigworth, 1983) and found to be insignificant (Mak and Webb, 1995b) because of the very low rate of conductance state transition under our experimental conditions (Fig. 2).

Because of the low applied potentials in our experiments ($|V_{ap}| < 80$ mV), $qe_0V_{ap} \approx kT$ (qe_0 is the charge on individual ions), so that the standard Schottky's formula (Schottky, 1918) of $2qe_0i_n^{ch}$ (i_n^{ch} is the current passing through the channel in conductance state n) for the shot-noise PSD is not applicable. Following our molecular model, shot noise arises from the discrete movement of ions over the energy barrier caused by the channel constriction. The ions take $\sim 3 \times 10^{-11}$ s to move across the constriction by electrodiffusion. The rate of ions moving across the channel is $\sim 1 \times 10^9$ s^{-1} from the channel current magnitude in our experiment ($|i_n^{ch}| < 0.2$ nA). Thus ions move singularly and effectively independently across the constriction, seeing no other ions when they are in the constriction. The independent, bidirectional transport of monovalent cations and anions across the channel constriction generates shot noise with current PSD $[S_i]_n^s$:

$$[S_i]_n^s = 2e_0i_n^{ch} \coth(v/2), \tag{27}$$

where $v = e_0V_{ch}/kT$, and V_{ch} is the potential drop across the channel constriction (Laüger, 1975). For $v \gg 1$, $\coth(v/2) \rightarrow 1$, Eq. 27 becomes Schottky's formula. At the low applied potential limit, $v \rightarrow 0$, $\coth(v/2) \rightarrow 2/v$, Eq. 27 then gives the familiar formula for Johnson noise (Nyquist, 1928): $[S_i]_n^s = 4kTi_n^{ch}/V_{ch} = 4kT/R_n^{ch}$, where R_n^{ch} is the resistance of the channel constriction.

Besides shot noise in the channel constriction, the noise in the spreading resistance around the constriction must also be taken into consideration. The spreading resistance is assumed to be ohmic with no discrete movement of ions in the electrolyte, so the noise is simple Johnson noise. The continuous medium approximation is used in the bulk electrolyte outside the channel as well as the wider vestibules of the channel on both sides of the constriction, and electroneutrality with complete correlation of cation and anion concentration fluctuations was assumed in these regions. Because the constriction resistance is in series with the spreading resistance, fluctuation in potential across the constriction due to shot noise and fluctuation in the potential across the spreading resistance due to Johnson noise are independent. Combined as described by Mak and Webb (1995b), the current PSD due to Johnson and shot noises $[S_i]_n^{J\&s}$ is

$$[S_i]_n^{J\&s} = e_0c_ni_n^{ch}[(1 - c_n)v \coth^2(v/2) + 2c_n \coth(v/2)], \tag{28}$$

where c_n is the fraction V_{ch}/V_{ap} and is derived from the i_n^{ch} versus V_{ap} relation for the various conductance states of the alamethicin channel (Mak and Webb, 1995a). These Johnson and shot noises can be detected as current noises, even in systems in equilibrium ($V_{ap} = 0$), with no net current flowing through (from Eq. 28, as $V_{ap} \rightarrow 0$, $[S_i]_n^{J\&s} \rightarrow 4kTi_n^{ch}/V_{ap} = 4kT/R$, where R is the total resistance of the channel, including the associated spreading resistance), and in systems whose conductance values are effectively constant, as those with very high charge carrier concentrations.

For a typical applied potential of about 40 mV (Fig. 4), the calculated shot and Johnson noises contribute about 20–40% of the total measured current noise in a persistent channel (Fig. 4 *A*). In a nonpersistent channel (Fig. 4 *B*), the measured current noise varies greatly in different conductance states, with shot and Johnson noises contributing from 9% (in lower conductance states) to 90% (in the highest conductance states) of the total measured current noise (Mak and Webb, 1995b).

The remaining current noise must be caused by fluctuations in the conductance of the channel, partly because of fluctuations in the conductivity of the electrolyte generated by ion concentration fluctuations and partly because of thermal molecular motions of the alamethicin polypeptides affecting the channel geometry. Such noise is directly proportional to $(i_n^{ch})^2$ (Fig. 4 *C*), as suggested by theory (Mak and Webb, 1995b).

Theoretical predictions and experimental observations

According to our theoretical derivation, the frequency dependence of the current noise PSD due to ion concentration

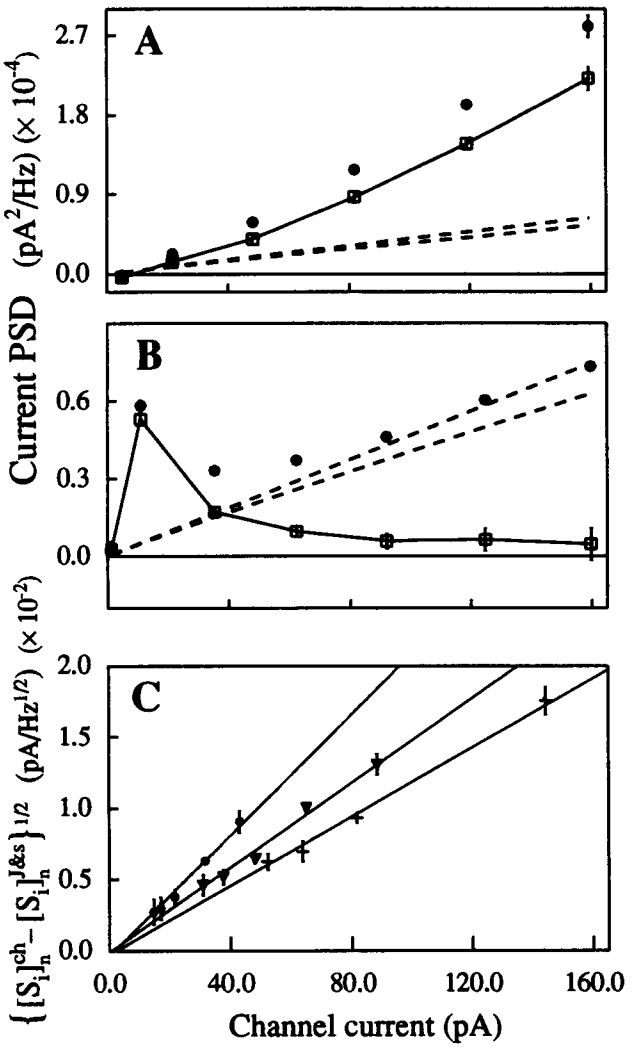

FIGURE 4 Graphs of current PSD versus mean channel current i_n^{ch} for (*A*) persistent channel and (*B*) nonpersistent channel, showing the calculated contribution of the Johnson and shot noises to the total measured current noise, with each point referring to a different conductance state under the same applied potential (+44 mV for *A* and +37 mV for *B*). Filled circles are total channel current PSD $[S_i]_n^{ch}$. The dashed lines indicate the range of the calculated current PSD due to Johnson and shot noises $[S_i]_n^{J\&s}$. The range arises from the uncertainty in estimating the value of c_n from the experimental channel current-voltage relation (Mak and Webb, 1995a). Open squares connected by the solid line are the difference: $[S_i]_n^{ch} - [S_i]_n^{J\&s}$, which is the excess noise consisting of the sum of contributions arising from ion concentration fluctuations and thermal molecular motions in the channels (Mak and Webb, 1995b). The magnitudes of the two contributions vary greatly among various conductance states of persistent and nonpersistent channels. Separation of the two contributions was described by Mak and Webb (1995b). (*C*) Graphs of $\sqrt{[S_i]_n^{ch} - [S_i]_n^{J\&s}}$ versus i_n^{ch} at various V_{ap} (29–80 mV) for individual persistent channel conductance states 2 (*circles*), 3 (*triangles*), and 4 (*crosses*) show the expected quadratic dependence of excess noise on mean channel current i_n^{ch}. One data point for each distinct channel conductance state was obtained from one experiment during which V_{ap} was kept constant. Data points from five different experiments were plotted in *C*. The straight lines are best fits to the data, assuming that $\sqrt{[S_i]_n^{ch} - [S_i]_n^{J\&s}} \propto i_n^{ch}$. The buffer NaCl concentration was 1.0 M for all data.

fluctuations is scaled by the reference frequency ω_0 (Eqs. 23 and 26). According to Eq. 19, $f_0 = \omega_0/2\pi \approx 2.5$ GHz, with ionic diffusion coefficient $D \approx 2 \times 10^{-9}$ m^{2}s^{-1} for an aqueous solution, and $\varepsilon \sim 5$ Å for a relatively large ion channel like an alamethicin channel in a high conductance state. Within our observable frequency range of 100 Hz to 20 kHz, $\hat{\omega} = \sqrt{f/f_0} \approx (0.1\text{–}3.0) \times 10^{-3}$, so $S_I(\omega) \approx S_I(0)$. This agrees with the experimental observation that the channel current noise spectra for all conductance states are nearly white, with little frequency dependence (Fig. 3).

After the Johnson and shot noise contributions calculated from our model (Mak and Webb, 1995b) were subtracted from the measured channel current noise, the remaining current noise PSD $[\Delta S_i]_n$ (averaged over 100 Hz to 20 kHz) is caused by fluctuations in the channel conductance. $[\Delta S_i]_n$ found from experimental data is proportional to $(i_n^{ch})^2$, so that the normalized noise PSD $[\Delta S_i]_n/(i_n^{ch})^2$ is voltage and current independent (within error limits of 5–30% for most persistent states and lower nonpersistent states) in our range of applied potential and channel current measured (Mak and Webb, 1995b). $[\Delta S_i]_n/(i_n^{ch})^2$ has a component S_n^{ion} due to fluctuations in the conductivity of the electrolyte in and around the channel caused by ion concentration fluctuations via random ion diffusion (Bezrukov and Vodyanoy, 1991 and 1994), and a component S_n^{mol} due to fluctuations in the shape and size of the channel pore caused by thermal excitation of the channel molecular structure (Stevens, 1972; Sigworth, 1985; Laüger, 1985). Whereas S_n^{mol} should have no direct dependence on the mean electrolyte concentration $\bar{\rho}$, S_n^{ion} is expected to be inversely proportional to $\bar{\rho}$, regardless of the geometry of the ion channel system (Eq. 9). Thus the dependence of $[\Delta S_i]_n/(i_n^{ch})^2$ on buffer concentration $\bar{\rho}$ should allow the two contributions to be separated:

$$\frac{[\Delta S_i]_n}{(i_n^{ch})^2} = S_n^{ion} + S_n^{mol} = \frac{G_n}{D\bar{\rho}} + S_n^{mol}, \qquad (29)$$

where G_n is the geometric factor controlled by the shape and size of the channel (cf. Eqs. 23 and 26).

Fig. 5 shows the graphs of normalized noise PSD $[\Delta S_i]_n/(i_n^{ch})^2$ versus $1/\bar{\rho}$ for selected nonpersistent channel conductance states. Within experimental error limits, the linear relation in Eq. 29 holds for buffer NaCl concentration between 0.33 and 2.0 M. The value of the slope α_n of the graph for conductance state n indicates the magnitude of the noise caused by electrolyte concentration fluctuations. According to Eq. 29,

$$\alpha_n = G_n/D. \qquad (30)$$

The slopes α_n for persistent channels were found with a similar procedure.

Fig. 6 shows the slopes α_n for various persistent and nonpersistent channel states plotted against the channel conductance values Λ_n in 1.0 M NaCl buffer solution. Fewer values of α_n were found for persistent channels because persistent channels occurred in less than 5% of our experiments (Mak and Webb, 1995a).

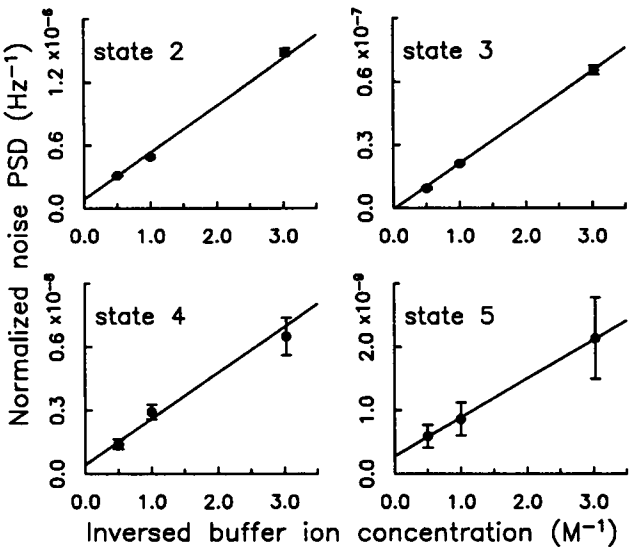

FIGURE 5 Graphs of the normalized noise PSD $[\Delta S_i]_n/(i_n^{ch})^2$ (Hz^{-1}) versus the inverse buffer ion concentration $1/\bar{p}$ (M^{-1}) for various nonpersistent channel conductance states.

Theoretical estimate α^{th} of the slope can be found using the simple geometric models of the channels described in the previous section. Equation 23 gives α^{th} for the contact disc model, whereas Eq. 26 gives α^{th} for the tube model. Because our experimental frequency range is $\ll f_0$, we use the value of $S^{ion}(\omega = 0)$. The appropriate channel dimension ε used in the equations is evaluated from the channel conductance Λ_n (Holm, 1967). The channel length ℓ assumed in the tube model is 35 Å (Schwarz and Savko, 1982). The theoretical estimates α^{th} from the two models were also plotted in Fig. 6. In the range of channel dimension shown in Fig. 6, $\varepsilon \approx a$, so the physical cut-off we used for the integral ($Q > 2a/\varepsilon$) has a large effect, especially for small pore radius ε. In the tube model, this causes the theoretical slopes α^{th} (*dotted line*) to increase less rapidly with a decrease in ε than would be expected from simple scaling. In the contact disc model, the high electric field density at the vicinity of the disc magnifies the effect of the physical cut-off, so that the calculated α^{th} actually decreases with a decrease in ε, instead of increasing with a decrease in ε in the simple scale law expected from Eq. 23.

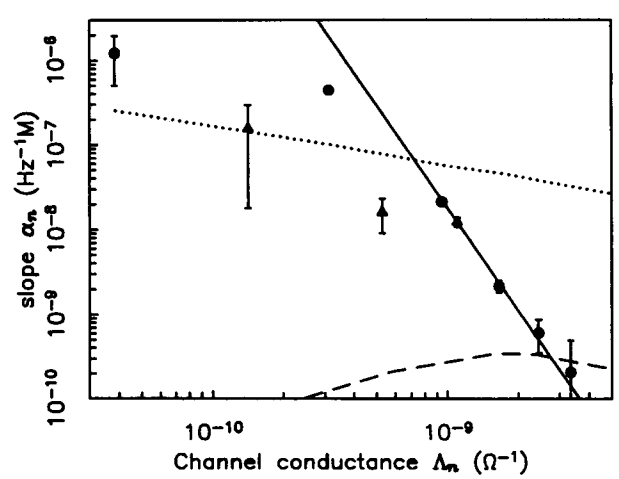

FIGURE 6 Graph of the slope α_n for alamethicin channels in various conductance states versus the channel conductance Λ_n in 1.0 M NaCl buffer solution at 7°C. Circles are α_n for nonpersistent channels (states 1–6). Triangles are α_n for persistent channels (states 1–3). The dashed line denotes α^{th}, estimated using the contact disc model. The dotted line denotes α^{th}, estimated using the tube model. The solid line represents the empirical relation $\alpha_n = \gamma(\Lambda_n)^{-4}$.

In Fig. 6 it can be seen that the theoretical estimate α^{th} from the contact disc model agrees with α_n found from experimental data at the higher conductance states (states 5 and 6) when the channel pore radius is large. This is expected because the contact disc model assumes that the thickness of the bilayer is negligible compared to the channel pore size. This assumption holds for large channels. However, departure from the contact disc model only occurs in conductance states below state 5, when the equivalent radius of the channel (Mak and Webb, 1995a) becomes smaller than 3 Å, much smaller than the thickness of the lipid bilayer and the full length of the alamethicin channel (35 Å). The equivalent radius of the channel is defined as the size of the channel pore at the channel constriction (Mak and Webb, 1995a). Because of the hourglass shape of the alamethicin channel pore, the pore radius at the mouth of the channel is much wider. Furthermore, the shape of the alamethicin channel concentrates the electric field in the vestibule toward the channel constriction, so that the electric field outside the channel constriction resembles that around a contact disc reasonably well, even for a relatively small channel.

For conductance state 1 of the persistent channels, the theoretical estimate α^{th} from the tube model agrees with the measured value of α_1. This indicates that in lower conductance states, as expected, the geometry of the channel resembles more closely a long electrolyte tube.

In the lowest two nonpersistent channel conductance states, the measured values of α_n are nearly an order of magnitude higher than those for persistent channels of comparable conductance value. This probably reflects the difference between the geometries of nonpersistent and persistent channels (Mak and Webb, 1995a). The arrangement of alamethicin molecules in nonpersistent channels may create regions in the channel pore in which the movement of ions is very restricted. This can reduce the effective diffusion coefficient D of the ions inside the channel (Levitt, 1974; Levitt and Subramanian, 1974), thus increasing α_n. However, this effect cannot be quantified because of the lack of structural information about nonpersistent channels. Apparently the difference between persistent and nonpersistent channel geometries decreases in higher conductance states, so that by state 3, α_3 values for persistent and nonpersistent channels are not very different.

The discrepancy between the theoretical estimate α^{th} from the tube model and the measured value of α_n in extremely small channels (nonpersistent state 1 channels) is

probably due to the fact that the continuous medium assumption we used in our modeling is no longer applicable for channels with equivalent channel radius $\varepsilon \ll 2a$.

In higher conductance states ($n > 2$), α_n values for both persistent and nonpersistent channels appear to vary with the channel conductance as

$$\alpha_n = \gamma(\Lambda_n)^{-4}, \tag{31}$$

where γ is $1.2 \times 10^{-44}\ \Omega^{-4}\mathrm{Hz}^{-1}\mathrm{M}$ from a least-squares fit of the data points. This is a purely empirical relation, which reflects the decrease in G_n as Λ_n increases, because of both the direct effect of the increase in channel pore size ε (Eqs. 23 and 26) and a change in the geometry of the channel (from resembling a tube to a contact disc) as the pore size increases.

As seen in Fig. 6, the experimentally obtained values of α_n for alamethicin channels in most conductance states (except the lowest two nonpersistent states) lie within the limits calculated from our simple geometric models of the channel. Even though the detailed variation of α_n with channel conductance Λ_n cannot be calculated from first principles, the trend agrees with predictions from our theoretical consideration: α_n for small channels in low-conductance states are close to the theoretical values α^{th} given by the tube model; whereas α_n for large channels in higher conductance states are close to values from the contact disc model. Considering the vast simplifications used in our theoretical derivation, the agreement between theoretical estimates and experimental results is remarkable and indicates that the models used in our theoretical consideration, although extremely simple, are not without merit. To fully account for the channel current noise due to ion concentration fluctuations, the intrinsic electric fields of the ion channel and the lipid bilayer should be properly taken into consideration; and more realistic boundary conditions for ion diffusion should be applied to find the Green's function. Sophisticated modeling on such a level is too complicated for analytical approach and probably has to rely on numerical simulations.

SUMMARY

In this paper we examined fluctuations in the conductance of an electrolyte system caused by ion concentration fluctuations via random ion diffusion. A Green's function approach similar to that used in fluorescence correlation spectroscopy was developed from first principles to evaluate the power spectral density of such fluctuations.

We applied this analytical Green's function approach to two simple geometric models of transmembrane ion channels: 1) The contact disc model, in which the channel is approximated by a circular hole in an infinitesimally thin membrane, gives the limit for large channels in which ion concentration fluctuations in the spreading resistance around the channel dominate. 2) The tube model, in which the channel is considered as an infinitely long tube of electrolyte, gives the limit for small channels in which ion concentration fluctuations inside the channel pore dominate.

The predictions of the theoretical models were compared with experimental data obtained from single-channel current measurement of alamethicin channels made by patch-clamp techniques. Alamethicin channels have multiple conductance states corresponding to different channel pore sizes. Excess noise in the channel current caused by ion concentration fluctuations via diffusion was observed above the Johnson and shot-noise levels.

Despite the simplicity of our models, two fundamental characteristics of the channel current noise due to ion concentration fluctuations predicted by both channel models agree well with experimental observations: 1) For frequencies $f \ll f_0 = 2D/2\pi\varepsilon^2 \approx 2.5$ GHz (Eqs. 18 and 19), which includes our observable frequency range, the current power spectral density due to ion concentration fluctuations is frequency independent, not $\propto 1/f$ (Fig. 3). 2) The normalized noise power spectral density due to ion concentration fluctuations is inversely proportional to the buffer ion concentration (Eqs. 23 and 26 and Fig. 5).

Because of the complex multidimensional integration required in the evaluation of the resistance fluctuation power spectral density in both geometric models (Eqs. 22 and 25), and the necessity to exclude from our calculation ion concentration fluctuation generated from physically unrealistic situations involving interionic separation less than the ionic diameter, the magnitudes of the conductance fluctuation power spectral density according to the geometric models must be estimated numerically with a simple computer algorithm.

For most conductance states of alamethicin channels, the measured magnitude of the current noise due to ion concentration fluctuations lies within the limits derived from our simple geometric models. For large conductance states ($n = 5$ and 6), the actual configuration of the channel should be well described by the contact disc model, and the measured noise amplitude agrees well with the contact disc model estimates. For very large channels beyond the range of conductance states observed in our experiments, the contact disc model is expected to describe the channels well with the scaling relation of $S^{ion}(\omega) \propto$ (the channel conductance)$^{-1}$. For small conductance states, the measured noise amplitude deviates appreciably from the contact disc model estimates because the channel starts to resemble the tube model. For persistent state 1 and 2 channels, the measured amplitude agrees with the tube model estimates, as expected. The discrepancy between the measured noise amplitude and the tube model estimates for nonpersistent states 1 and 2 channels probably reflects differences in the geometry of the nonpersistent and persistent channels and the inapplicability of the continuous medium assumption to extremely small channels.

For the majority of the observed conductance states, the channel pore configuration is in transition from resembling the tube model to resembling the contact disc model and is not well described by either models. The normalized ion

concentration fluctuation noise amplitude $S^{ion}(\omega)$ was found empirically (Eqs. 29–31) to follow the relation $S^{ion}(\omega) \approx (1.2 \times 10^{-44}\ \Omega^{-4}\mathrm{Hz}^{-1}\mathrm{M})/(\Lambda^4\bar{\rho})$.

We would like to thank J. K. Foskett for help and support in the preparation of the manuscript. We are also grateful to L. Ma and R. Keolean for helpful discussions.

This work was supported by a grant from the Office for Naval Research (N00014-89J-1656) and by facilities of the Developmental Resource for Biophysical Imaging and Optoelectronics provided by the National Institutes of Health (P41-RR04224) and the National Science Foundation (DIR 8800278).

REFERENCES

Bezrukov, S. M., A. I. Irkhin, and A. I. Sibilev. 1987. An upper estimate for 1/*f* noise intensity in ionic conductors from experiments with a molecular microcontact. *Phys. Lett. A.* 123:477–480.

Bezrukov, S. M., M. A. Pustovoit, A. I. Sibilev, and G. M. Drabkin. 1989. Large-scale conductance fluctuations in solutions of strong electrolytes. *Phys. B.* 159:388–398.

Bezrukov, S. M., and I. Vodyanoy. 1991. Electrical noise of the open alamethicin channel. *In* Noise in Physical Systems and 1/*f* Fluctuations. T. Musha, S. Sato, and M. Yamamoto, editors. Ohmsha, Tokyo. 641–644.

Bezrukov, S. M., and I. Vodyanoy. 1994. Noise in biological membranes and relevant ionic systems. *In* Biomembrane Electrochemistry. M. Blank and I. Vodyanoy, editors. American Chemical Society, Washington, DC. 375–399.

Boheim, G. 1974. Statistical analysis of alamethicin channels in black lipid membranes. *J. Membr. Biol.* 19:277–303.

Cahalan, M., and E. Neher. 1992. Patch clamp techniques: an overview. *Methods Enzymol.* 207:3–14.

Carslaw, H. S., and J. C. Jaeger. 1948. Conduction of Heat in Solids. Clarendon Press, Oxford.

Cherry, R. J., D. Chapman, and D. E. Graham. 1972. Studies of the conductance changes induced in bimolecular lipid membranes by alamethicin. *J. Membr. Biol.* 7:325–344.

Colquhoun, D., and F. J. Sigworth. 1983. Fitting and statistical analysis of single-channel records. *In* Single-Channel Recording. E. Neher and B. Sakmann, editors. Plenum Press, New York and London. 191–263.

Creighton, J. H. 1944. Principles and Applications of Electrochemistry. I. Principles. John Wiley and Sons, New York. 92–96.

DeFelice, L. J. 1981. Introduction to Membrane Noise. Plenum Press, New York and London. 329–330.

Eisenberg, M., M. E. Kleinberg, and J. H. Shaper. 1977. Channels across black lipic membranes. *Ann. N.Y. Acad. Sci.* 303:281–291.

Elson, E. L., and D. Madge. 1974. Fluorescence correlation spectroscopy. I. conceptual basis and theory. *Biopolymers.* 13:1–27.

Elson, E. L., and W. W. Webb. 1975. Concentration correlation spectroscopy: a new biophysical probe based on occupation number fluctuations. *Annu. Rev. Biophys. Bioeng.* 4:311–334.

Feher, G., and M. B. Weissman. 1973. Fluctuation spectroscopy: determination of chemical reaction kinetics from the frequency spectrum of fluctuations. *Proc. Natl. Acad. Sci. USA.* 70:870–875.

Fox, R. O., Jr., and F. M. Richards. 1982. A voltage-gated ion channel model inferred from the crystal structure of alamethicin at 1.5 Å resolution. *Nature.* 300:325–330.

Gordon, L. G. M., and D. A. Haydon. 1976. Kinetics and stability of alamethicin conducting channels in lipid bilayers. *Biochim. Biophys. Acta.* 436:541–556.

Hamill, O. P., A. Marty, E. Neher, B. Sakmann, and F. J. Sigworth. 1981. Improved patch-clamp techniques for high-resolution current recording from cells and cell-free membrane patches. *Pflugers Arch. Eur. J. Physiol.* 391:85–100.

Holm, R. 1967. Electric Contacts: Theory and Application. Springer-Verlag, Berlin and New York. 9–20.

Honig, E. P. 1974. 1/*f*-noise of bodies of arbitrary shape and of point contacts. *Philips Res. Rep.* 29:253–260.

Hooge, F. N. 1969. 1/*f* noise is no surface effect. *Phys. Lett. A.* 29: 139–140.

Hooge, F. N. 1972. Discussion of recent experiments on 1/*f* noise. *Physica.* 60:130–144.

Hooge, F. N. 1976. 1/*f* noise. *Phys. B.* 83:14–23.

Hooge, F. N., and J. L. M. Gaal. 1971. Fluctuations with a 1/*f* spectrum in the conductance of ionic solutions and in the voltage of concentration cells. *Philips Res. Rep.* 26:77–90.

Hooge, F. N., and A. M. H. Hoppenbrouwers. 1969. Contact noise. *Phys. Lett. A.* 29:642–643.

Hoppenbrouwers, A. M. H., and F. N. Hooge. 1970. 1/*f* noise of spreading resistances. *Philips Res. Rep.* 25:69–80.

Jordan, P. C. 1986. Ion channel electrostatics and the shapes of channel proteins. *In* Ion Channel Reconstitution. C. Miller, editor. Plenum Press, London and New York. 37–55.

Latorre, R., and O. Alvarez. 1981. Voltage-dependent channels in planar lipid bilayer membranes. *Physiol. Rev.* 61:77–150.

Latorre, R., P. Labarca, and D. Naranjo. 1992. Surface charge effects on ion conduction in ion channels. *Methods Enzymol.* 207:471–501.

Laüger, P. 1975. Shot noise in ion channels. *Biochim. Biophys. Acta.* 413:1–10.

Laüger, P. 1985. Structural fluctuations and current noise of ionic channels. *Biophys. J.* 48:369–373.

Lax, M., and P. Mengert. 1960. Influence of trapping, diffusion and recombination on carrier concentration fluctuation. *J. Phys. Chem. Solids.* 14:248–267.

Levitt, D. G. 1974. A new theory of transport for cell membrane pores. I. General theory and application to red cell. *Biochim. Biophys. Acta.* 373:115–131.

Levitt, D. G., and G. Subramanian. 1974. A new theory of transport for cell membrane pores. II. Exact results and computer simulation (molecular dynamics). *Biochim. Biophys. Acta.* 373:132–140.

Madge, D., E. L., Elson, and W. W. Webb. 1972. Thermodynamic fluctuation in a reacting system—measurements by fluorescence correlation spectroscopy. *Phys. Rev. Lett.* 29:705–708.

Mak, D. D., and W. W. Webb. 1995a. Two classes of alamethicin transmembrane channels: molecular models from single-channel properties. *Biophys. J.* 69:2323–2336.

Mak, D. D., and W. W. Webb. 1995b. Molecular dynamics of alamethicin transmembrane channels from open-channel current noise analysis. *Biophys. J.* 69:2337–2349.

Morse, P. M., and H. Feshbach. 1953. Methods of Theoretical Physics. McGraw-Hill, New York, Toronto, and London.

Mueller, P., and D. O. Rudin. 1968. Action potentials induced in bimolecular lipid membranes. *Nature.* 217:713–719.

Nyquist, H. 1928. Thermal agitation of electric charge in conductors. *Phys. Rev.* 32:110–113.

Press, W. H., B. P. Flannery, S. A. Teukolsky, and W. T. Vetterling. 1987a. Numerical Recipes. Cambridge University Press, Cambridge. 381–454.

Press, W. H., B. P. Flannery, S. A. Teukolsky, and W. T. Vetterling. 1987b. Numerical Recipes. Cambridge University Press, Cambridge. 102–130.

Richardson, J. M. 1950. The linear theory of fluctuations arising from diffusional mechanisms—an attempt at a theory of contact noise. *Bell Syst. Tech. J.* 29:117–141.

Sakmann, B., and E. Neher. 1983. Geometric parameters of pipettes and membrane patches. *In* Single-Channel Recording. E. Neher and B. Sakmann, editors. Plenum Press, New York and London. 37–51.

Sansom, M. S. P. 1991. The biophysics of peptide models of ion channels. *Prog. Biophys. Mol. Biol.* 55:139–235.

Schottky, W. 1918. Über spontane Stromschwankungen in verschiedenen Elektrizitätsleitern. *Ann. Phys.* 57:541–567.

Schwarz, G., and P. Savko. 1982. Structural and dipolar properties of the voltage-dependent pore former alamethicin in octanol/dioxane. *Biophys. J.* 39:211–219.

Sigworth, F. J. 1985. Open channel noise. I. Noise in acetylcholine receptor currents suggests conformational fluctuations. *Biophys. J.* 47:709–720.

Stevens, C. F. 1972. Inferences about membrane properties from electrical noise measurements. *Biophys. J.* 12:1028–1047.

Vandamme, L. K. J. 1976. On the calculation of 1/*f* noise of contacts. *Appl. Phys.* 11:89–96.

van Vliet, K. M., and J. R. Fassett. 1965. Fluctuations due to electronic transitions and transport in solids. *In* Fluctuation Phenomena in Solids. R. E. Burgess, editor. Academic Press, New York. 267–354.

Weissman, M. B. 1975. A mechanism for 1/*f* noise in diffusing membrane channels. *Phys. Rev. Lett.* 35:689–692.

Weissman, M. B. 1981. Fluctuation spectroscopy. *Annu. Rev. Phys. Chem.* 32:205–232.

Weissman, M. B. 1988. 1/*f* noise and other slow, nonexponential kinetics in condensed matter. *Rev. Mod. Phys.* 2:537–571.

Weissman, M. B., H. Schindler, and G. Feher. 1976. Determination of molecular weights by fluctuation spectroscopy: application to DNA. *Proc. Natl. Acad. Sci. USA.* 73:2776–2780.

Woolley, G. A., and B. A. Wallace. 1992. Model ion channels: gramicidin and alamethicin. *J. Membr. Biol.* 129:109–136.